

Magnetic phase transition of stage-2 $\text{Cu}_c\text{Co}_{1-c}\text{Cl}_2$ -graphite intercalation compounds

Masatsugu Suzuki, Itsuko S. Suzuki, Mitchell D. Johnson, Jaime Morillo, and Charles R. Burr
Department of Physics, State University of New York at Binghamton, Binghamton, New York 13902-6000

(Received 7 January 1994; revised manuscript received 14 March 1994)

Stage-2 $\text{Cu}_c\text{Co}_{1-c}\text{Cl}_2$ -graphite intercalation compounds (GIC's) ($0 \leq c \leq 1$) provide ideal two-dimensional random spin systems with a spin frustration effect arising from competing ferromagnetic and antiferromagnetic interactions. The magnetic properties of these compounds have been studied by dc and ac magnetic susceptibility, and superconducting quantum interference device magnetization. The sign of the Curie-Weiss temperature changes from positive to negative with increasing concentration around $c=0.80$ to 0.85 . The intraplanar exchange interaction $J(\text{Cu-Co})$ between Cu^{2+} and Co^{2+} spins is ferromagnetic and depends on the Cu concentration. These systems with $c < 0.9$ undergo a ferromagnetic phase transition at the critical temperature T_c . The irreversible effect of magnetization is observed below T_c . The low-temperature phase below T_c may correspond to a cluster glass phase where the spin direction of ferromagnetic clusters is frozen because of frustrated interisland interactions which include a dipole-dipole interaction and an interplanar antiferromagnetic interaction. The critical temperature T_c increases as c increases and exhibits a broad maximum around $c=0.5$. This enhancement of T_c is partly due to the ferromagnetic interaction $J(\text{Cu-Co})$. No magnetic phase transition is observed for $0.9 < c < 1$ partly because of the spin frustration effects arising from (i) the competition between ferromagnetic $J(\text{Cu-Co})$ and antiferromagnetic $J(\text{Cu-Cu})$ interactions, and (ii) the fully frustrated nature of the antiferromagnet on the triangular lattice.

I. INTRODUCTION

Recently the magnetic properties of magnetic random-mixture graphite intercalation compounds (RMGIC's) such as $\text{Co}_c\text{Ni}_{1-c}\text{Cl}_2$ GIC's,¹⁻³ $\text{Co}_c\text{Mn}_{1-c}\text{Cl}_2$ GIC's,^{3,4} $\text{Ni}_c\text{Mn}_{1-c}\text{Cl}_2$ GIC's,^{3,5} and $\text{Co}_c\text{Mg}_{1-c}\text{Cl}_2$ GIC's,^{6,7} have received considerable attention. The dimension of these systems can be decreased through intercalation by increasing the stage number, that is, the number of graphite layers between magnetic intercalate layers. Two kinds of magnetic ions are randomly distributed on the same intercalate layer. These RMGIC's may provide model systems for studying two-dimensional (2D) random-spin systems with various kinds of spin frustration effects such as competing ferromagnetic and antiferromagnetic interactions, and competing spin anisotropies between Ising, XY , and Heisenberg symmetries.

In this paper we are interested in the structural and magnetic properties of stage-2 $\text{Cu}_c\text{Co}_{1-c}\text{Cl}_2$ GIC's ($0 \leq c \leq 1$), where the $\text{Cu}_c\text{Co}_{1-c}\text{Cl}_2$ intercalate layers are separated by two graphite layers along the c axis. The Cu^{2+} ion is a magnetic Jahn-Teller ion and the Co^{2+} ion is a magnetic non-Jahn-Teller ion. These ions are assumed to be randomly distributed over the same intercalate layer. The intraplanar exchange interaction between Cu^{2+} spins is antiferromagnetic, while the intraplanar exchange interaction between Co^{2+} spins is ferromagnetic. For $c=0$, the stage-2 CoCl_2 GIC magnetically behaves like a 2D Heisenberg ferromagnet (fictitious spin $S=\frac{1}{2}$) with larger XY anisotropy.⁸⁻¹² The Co^{2+} ions form a triangular lattice with side $a=3.55 \text{ \AA}$. The spin Hamiltonian for Co^{2+} ions is described by the intraplanar exchange interaction ($J=7.75 \text{ K}$), the anisotropic exchange interaction J_A ($J_A/J=0.48$) showing XY an-

isotropy, and the antiferromagnetic interplanar exchange interaction J' . The antiferromagnetic interplanar exchange interaction is very weak compared to the intraplanar exchange interaction: $|J'|/J=8 \times 10^{-4}$. This compound shows two magnetic phase transitions at $T_{cu}=9.1 \text{ K}$ and $T_{cl}=8.0 \text{ K}$. Above T_{cu} , the system is in the paramagnetic phase. In the intermediate phase between T_{cl} and T_{cu} , the system has 2D spin ordering. There is no spin correlation between adjacent CoCl_2 layers. This 2D nature is characteristic of stage-2 and higher stage CoCl_2 GIC's. Below T_{cl} the 3D antiferromagnetic phase occurs: the 2D ferromagnetic layers are antiferromagnetically stacked along the c axis. For $c=1$, the stage-2 CuCl_2 GIC magnetically behaves like a 2D Heisenberg antiferromagnet on an isosceles triangular lattice with one short side ($a_1=3.30 \text{ \AA}$) and two longer sides ($a_2=3.72 \text{ \AA}$).¹³⁻¹⁸ In spite of this lattice distortion, which may arise due to the Jahn-Teller effect, the exchange interaction between nearest neighbor Cu^{2+} spins along the a_1 axis (J_1) is assumed to be the same as that between nearest-neighbor Cu^{2+} spins along the a_2 axis (J_2): $J_1=J_2=\langle J \rangle=-33.6 \text{ K}$. The susceptibility of stage-2 CuCl_2 GIC exhibits a broad peak of magnitude χ_{max} at the temperature T_{max} : $\chi_{\text{max}}=3.014 \times 10^{-3} \text{ emu/Cu mol}$ and $T_{\text{max}}=62 \text{ K}$.¹⁸ These values of χ_{max} and T_{max} can well be explained in terms of the theory of the susceptibility of a 2D Heisenberg antiferromagnet. No magnetic phase transition is observed either by dc magnetic susceptibility down to 1.5 K or by magnetic neutron scattering down to 0.3 K ,¹⁸ due to the spin frustration effect arising from the fully frustrated nature of the antiferromagnet on the triangular lattice.

For Cu concentration close to $c=0$, Cu^{2+} ions may be located on a triangular lattice with sides $a=3.55 \text{ \AA}$. The

nearest-neighbor (NN) distance between Cu^{2+} and Co^{2+} ions is 3.55 Å. The crystal field, which these Cu^{2+} ions feel, may be very different from the crystal field that Cu^{2+} ions feel in stage-2 CuCl_2 GIC. For Cu concentration close to $c = 1$, Co^{2+} ions may be located on an isosceles triangular lattice. The NN and next nearest neighbor (NNN) distances between Co^{2+} and Cu^{2+} ions are a_1 and a_2 , respectively. The crystal field, which these Co^{2+} ions feel, may be very different from the crystal field that Co^{2+} ions feel in stage-2 CoCl_2 GIC. Thus, the nature of the intraplanar exchange interaction between Cu^{2+} and Co^{2+} ions, $J(\text{Cu-Co})$, may drastically change with Cu concentration. Furthermore, in the intermediate Cu concentration, spin frustration effect is expected to occur because of the competition between antiferromagnetic and ferromagnetic intraplanar exchange interactions. This spin frustration effect may lead to a cluster-glass or spin-glass behavior.

We have succeeded in synthesizing well-defined stage-2 $\text{Cu}_c\text{Co}_{1-c}\text{Cl}_2$ GIC's. Here we will present our experimental results on dc and ac magnetic susceptibility, and superconducting quantum interference device (SQUID) magnetization measurements of stage-2 $\text{Cu}_c\text{Co}_{1-c}\text{Cl}_2$ GIC's based on single-crystal kish graphite (SCKG) and highly oriented pyrolytic graphite (HOPG). The Cu concentration dependence of the Curie-Weiss temperature is discussed in terms of molecular-field theory. We will show from this comparison that the interaction $J(\text{Cu-Co})$ is ferromagnetic and increases with increasing Cu concentration. We will also show that stage-2 $\text{Cu}_c\text{Co}_{1-c}\text{Cl}_2$ GIC's with $c < 0.9$ undergo a ferromagnetic phase transition at the critical temperature T_c and that T_c increases with increasing concentration and shows a broad maximum around $c = 0.5$. This enhancement of T_c is partly due to the ferromagnetic interaction $J(\text{Cu-Co})$. We will present our data of SQUID magnetization for stage-2 $\text{Cu}_c\text{Co}_{1-c}\text{Cl}_2$ GIC's with $c \leq 0.87$ including the temperature dependence of zero-field-cooled (ZFC) magnetization and field-cooled (FC) magnetization. We will show that the ZFC magnetization deviates downward from the FC magnetization below a critical temperature T_c and shows a broad peak at a temperature T_{max} . The irreversible effect of the magnetization will be discussed in terms of a cluster-glass phase model,³ where the spin directions of ferromagnetic clusters are frozen due to frustrated interisland interactions.

II. EXPERIMENTAL PROCEDURE

The intercalants were prepared from reagent grade CuCl_2 and CoCl_2 powders. The powders were dehydrated at 400°C in the presence of HCl gas at one atmosphere. Fractions of these compounds were carefully massed and mixed together to create the concentrations of Co and Cu needed for our samples. Single crystals of $\text{Cu}_c\text{Co}_{1-c}\text{Cl}_2$ over the entire range of Cu concentrations were grown using the Bridgeman method: a mixture of dehydrated CuCl_2 and CoCl_2 with nominal weight composition was heated at 630–730°C in a quartz tube sealed in a vacuum. Two types of graphite were used to make

GIC samples. Stage-2 $\text{Cu}_c\text{Co}_{1-c}\text{Cl}_2$ GIC samples with $c \geq 0.4$ were synthesized by intercalation of single crystal $\text{Cu}_c\text{Co}_{1-c}\text{Cl}_2$ into HOPG: the mixture of HOPG and $\text{Cu}_c\text{Co}_{1-c}\text{Cl}_2$ was heated at 450°C for 14 days in Pyrex glass sealed in a vacuum. Stage-2 $\text{Cu}_c\text{Co}_{1-c}\text{Cl}_2$ GIC samples with $c < 0.4$ were synthesized by intercalation of single crystal $\text{Cu}_c\text{Co}_{1-c}\text{Cl}_2$ into SCKG: the mixture of SCKG and $\text{Cu}_c\text{Co}_{1-c}\text{Cl}_2$ was heated at 520°C for 20 days in the presence of chlorine gas at a pressure of 740 Torr.

The (00L) x-ray diffraction of stage-2 $\text{Cu}_c\text{Co}_{1-c}\text{Cl}_2$ GIC was measured at 300 K by using a Huber double circle diffractometer with a $\text{MoK}\alpha$ x-ray radiation source (1.5 kW) and HOPG monochromator. An entrance slit of $2 \times 2 \text{ mm}^2$ was placed between the monochromator and the sample. The x-ray beam diffracted by the sample was collimated using an exit slit of $1 \times 1 \text{ mm}^2$ and detected with a Bicron photomultiplier tube.

The concentration of stage-2 $\text{Cu}_c\text{Co}_{1-c}\text{Cl}_2$ GIC samples was determined by electron microprobe measurement. The measurement was carried out using a scanning electron microscope (Hitachi model S-450). Electrons having a kinetic energy of 20 keV penetrated the sample to a depth of the order of $2 \mu\text{m}$, and spread out to a similar distance. The quoted concentration is the averaged value of measurements over several different points in the sample.

The dc magnetic susceptibility of stage-2 $\text{Cu}_c\text{Co}_{1-c}\text{Cl}_2$ GIC's was measured using a Faraday balance in the temperature range between 1.5 and 300 K. A quartz bucket containing the sample was suspended from a fine quartz fiber attached to Cahn electrobalance. A Hewlett Packard 6655A programmable dc power supply delivered current to a Varian 4004 electromagnet, which produced a magnetic field of up to 2 kOe. The temperature of the sample over the entire range of 1.5 to 300 K was measured using a DT-470-SD13 diode (Lake Shore).

The ac magnetic susceptibility of stage-2 $\text{Cu}_c\text{Co}_{1-c}\text{Cl}_2$ GIC's was measured using an ac Hartshorn bridge method in the temperature range between 2.6 and 20 K. An ac magnetic field of 330 Hz was applied in an arbitrary direction in the c plane of the samples. A Wavetek oscillator 188 generated a 330-Hz signal, which was fed to a primary coil surrounding the sample. The induced voltage created in a secondary coil was fed into a Princeton Applied Research 186A lock-in amplifier.

The highly sensitive measurements of magnetization in stage-2 $\text{Cu}_c\text{Co}_{1-c}\text{Cl}_2$ GIC's were carried out with a SQUID magnetometer (model VTS-905 SQUID system, manufactured by S.H.E. Corporation). The measurements were performed in three steps. (i) A sample having a weight of 4–7 mg was first cooled to a temperature of 4.2 K from 300 K in 5 min in the absence of any external magnetic field. A field of 1 Oe was then applied along any direction perpendicular to the c axis, and held constant, while the measurements were made from 4.2 to 20 K. (ii) The temperature dependence of zero-field-cooled (ZFC) magnetization M_{ZFC} was measured, while increasing the temperature from 4.2 to 20 K. (iii) The sample was again cooled in a field of 1 Oe and the temperature dependence of field-cooled (FC) magnetization M_{FC} was

measured while decreasing the temperature from 20 to 4.2 K.

III. RESULT

The Cu concentration of stage-2 $\text{Cu}_c\text{Co}_{1-c}\text{Cl}_2$ GIC samples was determined by weight-uptake and electron microprobe measurements. In weight-uptake measurements, the Cu concentration of GIC samples was determined by comparing the weight of pristine graphite before intercalation to its weight after intercalation. This is a very simple method, but it gives an average Cu concen-

tration of the GIC sample over the whole sample. In electron microprobe measurements, the actual Cu concentration of stage-2 $\text{Cu}_c\text{Co}_{1-c}\text{Cl}_2$ GIC's may be different from the concentration of the pristine compounds used as intercalants. When the electron beam bombards the sample surface, characteristic x rays of each element in the GIC are emitted. This x-ray intensity was analyzed by the energy dispersion method. The electron microprobe measurements were made for samples of stage-2 $\text{Cu}_c\text{Co}_{1-c}\text{Cl}_2$ GIC's with $c \geq 0.8$. Figure 1(a) shows the relationship between the bulk concentration c_b of intercalants and the concentration c_e for the stage-2 $\text{Cu}_c\text{Co}_{1-c}\text{Cl}_2$ GIC's, where c_e is the Cu concentration determined from the electron microprobe measurement. The data of c_e vs c_b agree with a straight line of $c_e = c_b$ in the Cu concentration range of $0.8 \leq c \leq 1$. Hereafter, we assume that the actual concentration c of GIC's is the same as the concentration of the pristine compounds used as intercalant. Figure 1(b) shows a typical example of (00L) x-ray-diffraction pattern for stage-2 $\text{Cu}_c\text{Co}_{1-c}\text{Cl}_2$ GIC's with $c = 0.8$. Sharp Bragg reflections are observed at the wave number $Q_c = (2\pi/d)L$, where L is an integer, and d is the c -axis repeat distance. A least-squares fit of the data of Q_c vs L to the relation $Q_c = (2\pi/d)L$ yields the value of d listed in Table I. Large experimental uncertainties in d are observed for the samples with $c = 0.95, 0.75, 0.70, 0.20$, and 0.10 . An analysis of (00L) x-ray-diffraction pattern for these compounds shows that the peak shift of Bragg reflection from that of pure stage-2 oscillates with the Bragg reflection index of stage-2, indicating that these compounds are dominantly stage-2 but have a Hendricks-Teller (HT)-type staging disorder along the c axis.^{19,20} In spite of large uncertainties in d , the c -axis repeat distance seems to be independent of the Cu concentration c : $d \approx 12.80 \text{ \AA}$.

The dc magnetic susceptibility for stage-2 $\text{Cu}_c\text{Co}_{1-c}\text{Cl}_2$ GIC samples listed in Table I was mea-

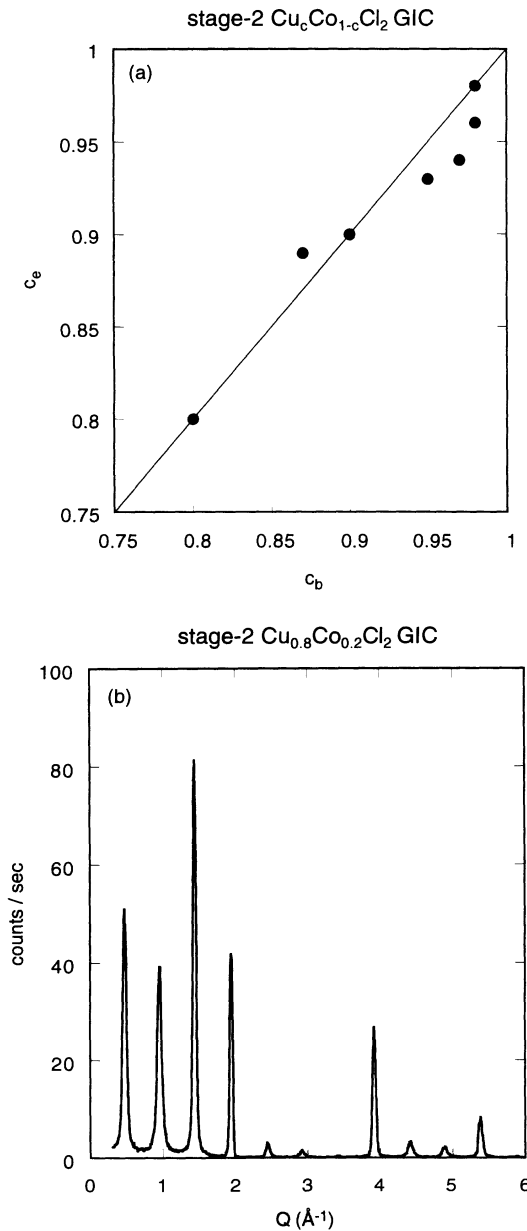


FIG. 1. (a) Relationship between the bulk concentration (c_b) of intercalant and the concentration (c_e) determined from electron microprobe measurements for stage-2 $\text{Cu}_c\text{Co}_{1-c}\text{Cl}_2$ GIC's in the Cu concentration range $0.80 \leq c \leq 1$. The straight line is described by $c_e = c_b$. (b) (00L) x-ray-diffraction patterns for stage-2 $\text{Cu}_c\text{Co}_{1-c}\text{Cl}_2$ GIC with $c = 0.80$. $Q_c = (2\pi/d)L$.

TABLE I. Θ , C_M , P_{eff} , and d spacing for stage-2 $\text{Cu}_c\text{Co}_{1-c}\text{Cl}_2$ GIC's.

c	Θ (K)	C_M (emu/av mol)	P_{eff} (μ_B)	d spacing (\AA)
1.0	-100.9	0.64	2.26	12.81±0.05
0.98	-71.71±1.44	0.73	2.42	12.85±0.01
0.97	-56.32±0.63	0.73	2.42	12.86±0.03
0.95	-42.22±0.23	0.71	2.38	12.85±0.12
0.93	-43.76±0.55	0.81	2.55	12.80±0.05
0.88	-0.32±0.32	1.29	3.22	
0.87	-4.40±0.31	0.76	2.47	12.80±0.05
0.85	-6.60±0.28	0.80	2.54	12.82±0.04
0.80	2.52±0.22	1.11	2.98	12.83±0.05
0.75	23.63±5.34	1.34	3.28	12.70±0.10
0.70	8.31±0.31	1.50	3.47	12.83±0.24
0.60	12.82±0.33	2.36	4.35	
0.50	14.48±1.35	1.70	3.69	12.83±0.05
0.40	19.19±0.28	2.02	4.02	
0.20	19.07±0.27	4.78	6.18	12.84±0.15
0.10	25.29±0.29	4.52	6.01	12.79±0.10
0	23.2	3.84	5.54	12.79±0.01

sured in the temperature range between 1.5 and 300 K. Figure 2(a) shows the temperature dependence of dc magnetic susceptibility for stage-2 $\text{Cu}_c\text{Co}_{1-c}\text{Cl}_2$ GIC's with $c = 0, 0.8, 0.87, 0.93, 0.98,$ and 1 , where an external field of 2 kOe is applied along any direction perpendicular to the c axis. For $c = 1$, the dc magnetic susceptibility shows a broad peak at $T_{\text{max}} = 62$ K. This broad peak completely disappears for $c = 0.98$. For $c \leq 0.98$, the dc magnetic susceptibility monotonically decreases with increasing temperature in the temperature range between 20 and 300 K. A least-squares fit of the susceptibility data to the Curie-Weiss law

$$\chi_M = \frac{C_M}{T - \Theta} + \chi_M^0, \quad (1)$$

in the temperature range between 150 and 300 K yields the values of C_M and Θ listed in Table I for each Cu concentration, where C_M is the Curie-Weiss constant, Θ is the Curie-Weiss temperature, and χ_M^0 is the temperature-independent susceptibility. Figure 2(b) shows the reciprocal susceptibility described by $(\chi_M - \chi_M^0)^{-1}$ vs temperature for stage-2 $\text{Cu}_c\text{Co}_{1-c}\text{Cl}_2$ GIC's with $c = 0, 0.8, 0.87, 0.93, 0.98,$ and 1 . All the data agree well with straight lines above 150 K, indicating that the susceptibility data obey the Curie-Weiss law. We find that the reciprocal susceptibility for $c = 1$ deviates greatly from the Curie-Weiss law below 100 K because of the growth of short-range spin order. Such a deviation from the Curie-Weiss law becomes small with decreasing Cu concentration and almost disappears for $c = 0.80$. Figure 3(a) shows the Cu concentration dependence of P_{eff} for stage-2 $\text{Cu}_c\text{Co}_{1-c}\text{Cl}_2$ GIC's. The effective magnetic moment P_{eff} seems to decrease monotonically with increasing Cu concentration. According to molecular field theory¹ the effective magnetic moment P_{eff} is predicted as

$$P_{\text{eff}} = [cP_{\text{eff}}^2(\text{Cu}^{2+}) + (1-c)P_{\text{eff}}^2(\text{Co}^{2+})]^{1/2}, \quad (2)$$

where $P_{\text{eff}}(\text{Cu}^{2+}) = 2.26\mu_B$ for stage-2 CuCl_2 GIC (Ref. 18) and $P_{\text{eff}}(\text{Co}^{2+}) = 5.51\mu_B$ for stage-2 CoCl_2 GIC.¹⁰ In Fig. 3(a) the solid line denotes the prediction described by Eq. (2). The data of P_{eff} vs c are in good agreement with the solid line except for $c = 0.1$ and 0.2 . This result indicates that (i) Cu and Co ions exist as divalent in the intercalate layers, and that (ii) the actual Cu concentration of GIC samples coincides with the Cu concentration of bulk intercalants. Figure 3(b) shows the Cu concentration dependence of Θ for stage-2 $\text{Cu}_c\text{Co}_{1-c}\text{Cl}_2$ GIC's. The Curie-Weiss temperature Θ monotonically decreases with increasing Cu concentration. The sign of Θ changes from positive to negative for $0.80 \leq c \leq 0.85$, indicating that the average intraplanar exchange interaction changes from ferromagnetic to antiferromagnetic. The value of Θ

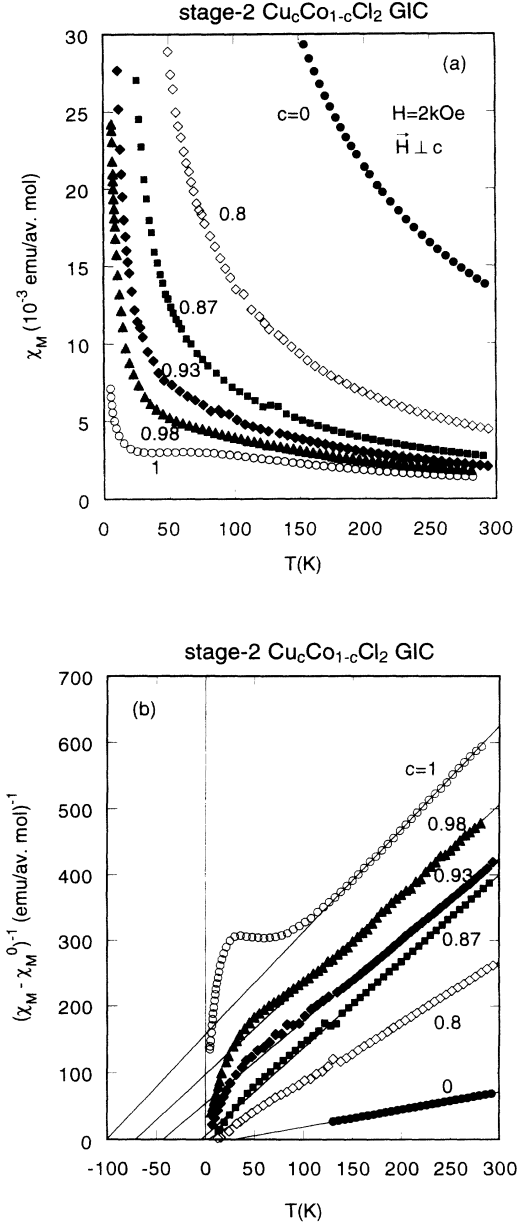


FIG. 2. (a) dc magnetic susceptibility vs temperature in stage-2 $\text{Cu}_c\text{Co}_{1-c}\text{Cl}_2$ GIC's with $c = 0, 0.8, 0.87, 0.93, 0.98,$ and 1 ; $H = 2$ kOe; $H \perp c$. (b) Reciprocal susceptibility $(\chi_M - \chi_M^0)^{-1}$ vs temperature in stage-2 $\text{Cu}_c\text{Co}_{1-c}\text{Cl}_2$ GIC's with $c = 0, 0.8, 0.87, 0.93, 0.98,$ and 1 . The straight lines obey the Curie-Weiss law.

drastically decreases with increasing Cu concentration for $c > 0.95$. Note that similar data of Θ vs c has been reported for $\text{Eu}_{1-c}\text{Gd}_c\text{Se}$,²¹ where Θ shows a broad peak around $c = 0.2$, and changes its sign from positive to negative around $c = 0.6$. The Cu concentration dependence of Θ is predicted from the molecular field theory¹ as

$$\Theta = \frac{c^2 P^2(\text{Cu})\Theta(\text{Cu}) + (1-c)^2 P^2(\text{Co})\Theta(\text{Co}) + 2ac(1-c)\sqrt{|\Theta(\text{Cu})\Theta(\text{Co})|}P(\text{Cu})P(\text{Co})}{cP^2(\text{Cu}) + (1-c)P^2(\text{Co})}, \quad (3)$$

where $\Theta(\text{Cu}) = -100.9$ K (Ref. 18) and $\Theta(\text{Co}) = 23.2$ K (Ref. 10) are the Curie-Weiss temperatures of stage-2 CuCl_2 GIC and stage-2 CoCl_2 GIC. The intraplanar exchange interaction between Cu^{2+} and Co^{2+} spins, $J(\text{Cu-Co})$, is defined as $J(\text{Cu-Co}) = \alpha [|J(\text{Cu-Cu}) J(\text{Co-Co})|]^{1/2} = 16.14\alpha [\text{K}]$, where $J(\text{Co-Co}) = 7.75$ K,¹⁰ $J(\text{Cu-Cu}) = -33.63$ K,¹⁸ and α is an undetermined parameter. We assume that $J(\text{Co-Co})$ and $J(\text{Cu-Cu})$ are independent of concentration. In Fig. 3(b) the relations of Θ vs c for $\alpha = 0, 1$, and 2 calculated from Eq. (3) are denoted as dash-dotted, dotted, and solid lines, respectively. We find that our data of Θ vs c coincide with the dash-dotted line for $0 \leq c \leq 0.2$, with the dotted line at $c \approx 0.7$, and with the solid line for $c \approx 0.8$. Figure 3(c) shows the Cu concentration dependence of α , which is calculated by substituting the value of Θ for each concentration into Eq. (3).

The parameter α is positive for any Cu concentration, and monotonically increases with increasing Cu concentration. The data of α vs c seem to fit with the solid lines denoted by an expression $\alpha = 3.59c^3$ for intermediate concentration. This relation may not be valid for low and high concentrations where the probability of finding Cu-Co pairs, $p(\text{Cu-Co})$, becomes very small. These results indicate that (i) $J(\text{Cu-Co})$ is ferromagnetic for any Cu concentration, and that (ii) $J(\text{Cu-Co})$ is larger than $J(\text{Co-Co})$ for $c > 0.51$ and larger than $|J(\text{Cu-Cu})|$ for $c > 0.83$, where the sign of Θ changes from positive to negative with increasing concentration. The concentration dependence of $J(\text{Cu-Co})$ may be related to the deformation of in-plane structure from an equilateral triangular lattice to an isosceles triangular lattice with increasing Cu concentration. Here we notice that the intraplanar

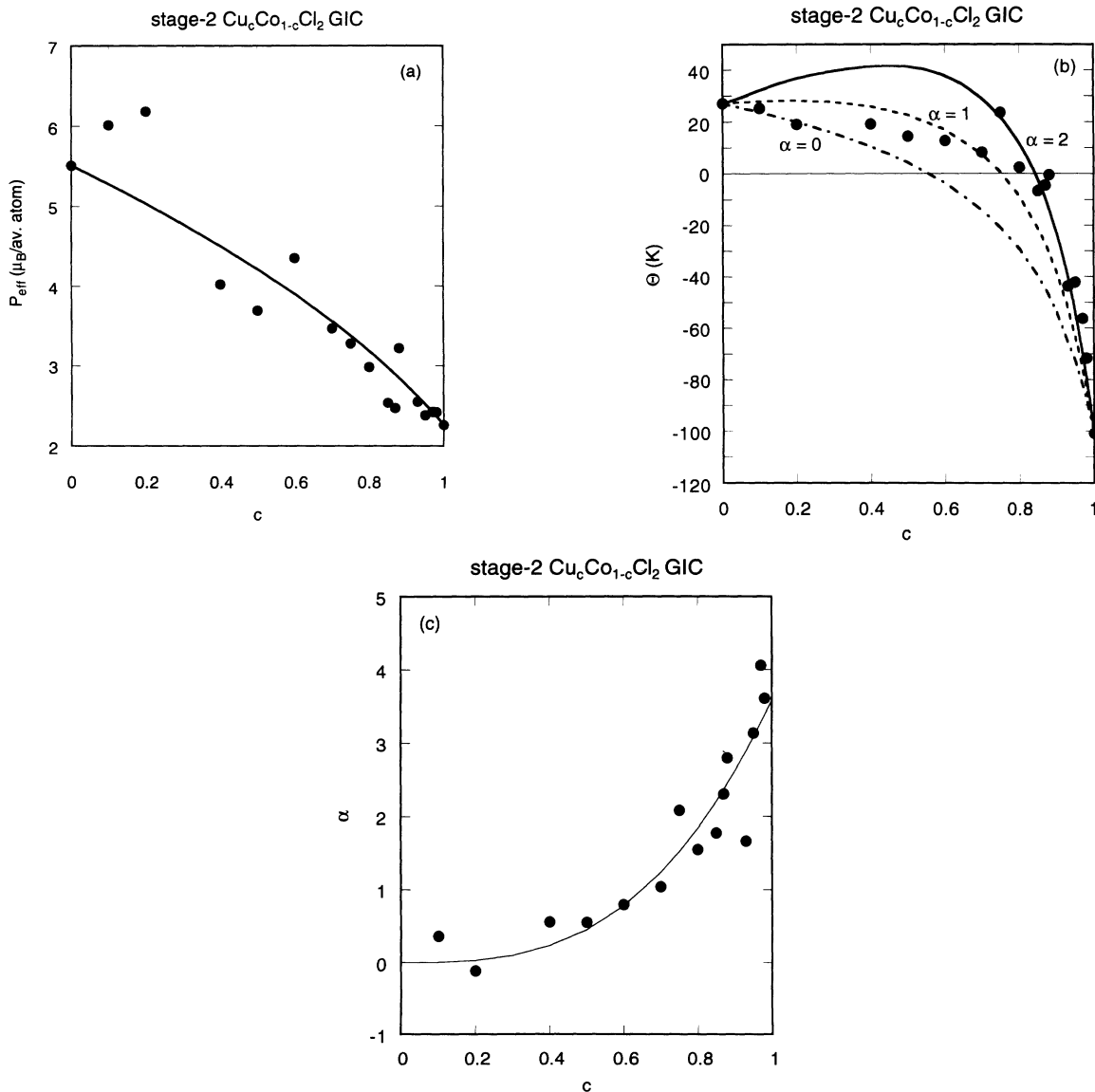


FIG. 3. (a) P_{eff} (μ_B /av atom) vs Cu concentration c in stage-2 $\text{Cu}_c\text{Co}_{1-c}\text{Cl}_2$ GIC's determined from high-temperature dc magnetic susceptibility. The solid line is denoted by Eq. (2). (b) Θ vs c in stage-2 $\text{Cu}_c\text{Co}_{1-c}\text{Cl}_2$ GIC's. The dash-dotted, dotted, and solid lines are denoted by Eq. (3) with $\alpha = 0, 1$, and 2, respectively. (c) α vs c in stage-2 $\text{Cu}_c\text{Co}_{1-c}\text{Cl}_2$ GIC's. The solid line is denoted by $\alpha = 3.59c^3$.

interactions $J(\text{Co-Ni})$ of stage-2 $\text{Co}_c\text{Ni}_{1-c}\text{Cl}_2$ GIC's,¹ $J(\text{Co-Mn})$ of stage-2 $\text{Co}_c\text{Mn}_{1-c}\text{Cl}_2$ GIC's,⁴ and $J(\text{Ni-Mn})$ of stage-2 $\text{Ni}_c\text{Mn}_{1-c}\text{Cl}_2$ GIC's⁵ are all ferromagnetic and independent of concentration: $J(\text{Co-Ni})=1.2 [J(\text{Co-Co})J(\text{Ni-Ni})]^{1/2}$, $J(\text{Co-Mn})=1.2 [J(\text{Co-Co})|J(\text{Mn-Mn})|]^{1/2}$, and $J(\text{Ni-Mn})=1.09 [J(\text{Ni-Ni})|J(\text{Mn-Mn})|]^{1/2}$. The in-plane structure of these compounds forms an equilateral triangular lattice and does not change with concentration. The origin of the ferromagnetic $J(\text{Cu-Co})$ will be discussed in Sec IV.

The dc magnetic susceptibility at low temperature is described by $\chi=M/H$, where M is the magnetization of the system. Figures 4(a) and 4(b) show the temperature dependence of M/H for stage-2 $\text{Cu}_c\text{Co}_{1-c}\text{Cl}_2$ GIC's with $c=0.1, 0.2, 0.4, 0.6, 0.7$, and 0.8 . A magnetic field of 100 Oe was applied along any direction perpendicular to the c axis. For $c \leq 0.5$ the magnetization drastically increases below the critical temperature T_c . The temperature

dependence of the magnetization M near T_c is described by a smeared power law with critical exponent β .¹ We assume a Gaussian distribution of the critical temperature with the average value $\langle T_c \rangle$ and width σ , which is described by

$$f(T_c) = \frac{1}{\sqrt{2\pi}\sigma} \exp \left[-\frac{1}{2} \left(\frac{T_c - \langle T_c \rangle}{\sigma} \right)^2 \right]. \quad (4)$$

The magnetization can then be expressed by a power law with a critical exponent β ,

$$M(T) = M(0) \int_T^\infty D \left[1 - \frac{T}{T_c} \right]^\beta f(T_c) dT_c, \quad (5)$$

where D is a constant. The values of β , $\langle T_c \rangle$, and σ are determined from a least-squares fit and are listed in Table II. Note that this method is not applicable to the magne-

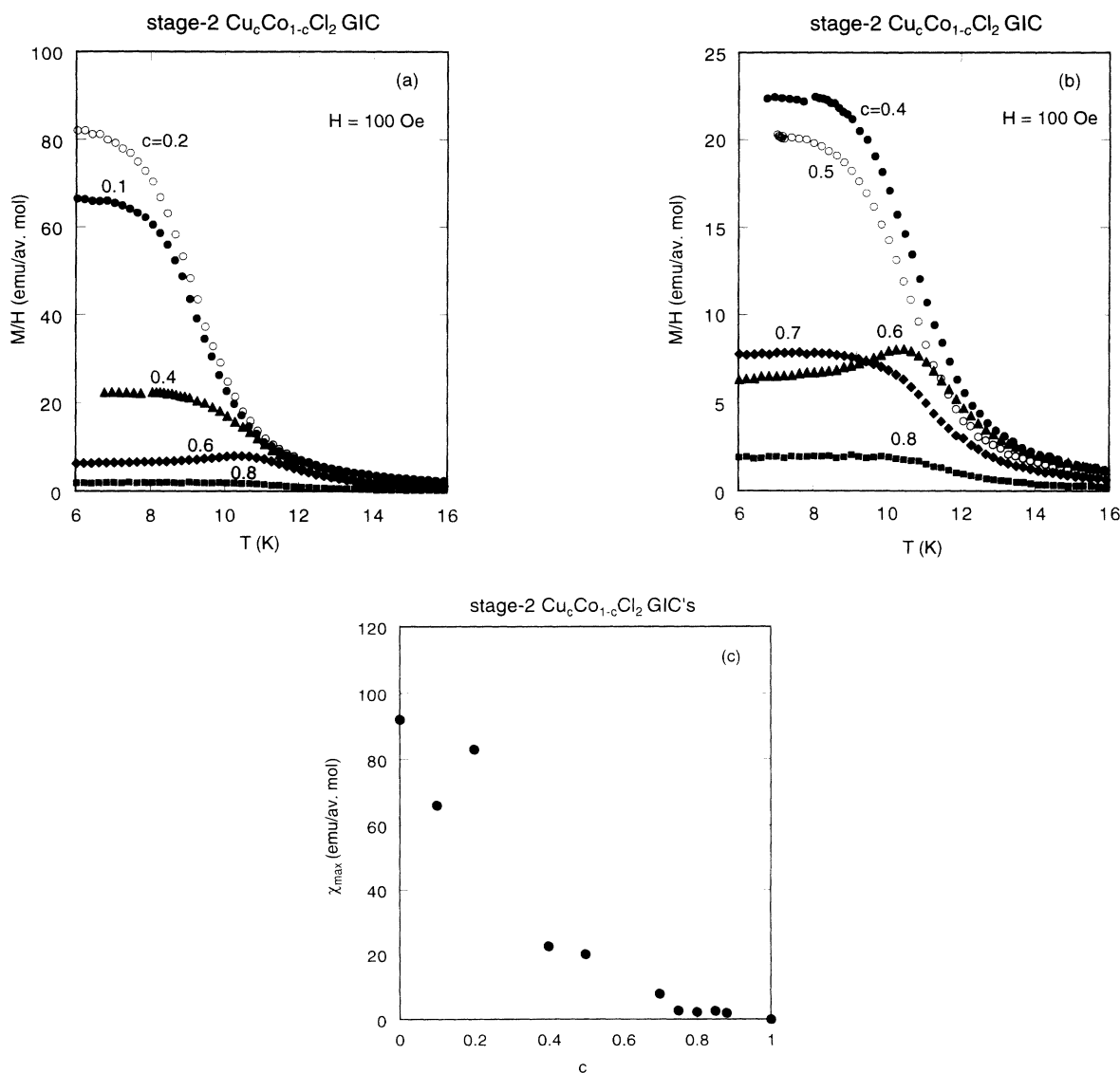


FIG. 4. (a) dc magnetic susceptibility vs temperature in stage-2 $\text{Cu}_c\text{Co}_{1-c}\text{Cl}_2$ GIC's with $c=0.1, 0.2, 0.4, 0.6$, and 0.8 at low temperatures; $H=100$ Oe; $H \perp c$. (b) dc magnetic susceptibility vs temperature in stage-2 $\text{Cu}_c\text{Co}_{1-c}\text{Cl}_2$ GIC's with $c=0.4, 0.5, 0.6, 0.7, 0.8$ at low temperatures; $H=100$ Oe; $H \perp c$. (c) Maximum susceptibility χ_{\max} vs Cu concentration c for stage-2 $\text{Cu}_c\text{Co}_{1-c}\text{Cl}_2$ GIC's.

TABLE II. T_c , $\langle T_c \rangle$, β , and σ for stage-2 $\text{Cu}_c\text{Co}_{1-c}\text{Cl}_2$ GIC's, which are determined from ac and dc magnetic susceptibility.

c	T_c (K)	$\langle T_c \rangle$ (K)	β	σ (K)
0.93				
0.90	9.40			
0.88	9.36	11.49	0.061	1.74
0.87	9.88			
0.85	10.18	11.87	0.035	1.74
0.80	10.22	11.80	0.058	1.53
0.75	10.66			
0.70	10.02			
0.60	9.72			
0.50	10.00	11.27	0.240	0.94
0.40	9.92	11.11	0.064	1.19
0.20	8.84	9.44	0.036	1.16
0.10	8.58	9.51	0.002	1.10
0	8.20	8.78	0.082	0.62

tization M for $c=0.6$ because of a cusplike behavior around T_c . The exponent β of stage-2 $\text{Cu}_c\text{Co}_{1-c}\text{Cl}_2$ GIC's is equal to 0.05 ± 0.03 except for $c=0.5$. This small value of β indicates that stage-2 $\text{Cu}_c\text{Co}_{1-c}\text{Cl}_2$ GIC's behave magnetically either as 2D XY-like or 2D Heisenberg-like spin systems. The value of β for 2D XY and 2D Heisenberg models is assumed to be much smaller than those for the 2D Ising model ($\beta=0.125$), the 3D Ising model ($\beta=0.326$), the 3D XY model ($\beta=0.345$), and the 3D Heisenberg model ($\beta=0.367$).²² Figure 4(c) shows a plot of maximum susceptibility χ_{\max} as a function of Cu concentration. The maximum susceptibility is found to drastically decrease with increasing Cu concentration: $\chi_{\max}=92$ emu/Co mol at $c=0$ and $\chi_{\max}=7.5 \times 10^{-3}$ emu/Cu mol at $c=1$. The large values of χ_{\max} for $0 \leq c \leq 0.2$ indicate that there exists a ferromagnetic long-range order of Co^{2+} spins in the intercalate layers. If Cu^{2+} ions are nonmagnetic ions, then the value of χ_{\max} is assumed to reduce to zero for $c > c_p$ in association with the disappearance of ferromagnetic long-range order, where c_p is the percolation threshold and equal to 0.5 for a triangular lattice.²³ As shown in Fig. 4(c), the value of χ_{\max} does not reduce to zero at $c=0.5$, but shows a taillike behavior even for $c > c_p$, indicating that a ferromagnetic long-range order still exists for $c > c_p$. The ferromagnetic interaction $J(\text{Cu-Co})$ contributes to this ferromagnetic long-range order, while the antiferromagnetic interaction $J(\text{Cu-Cu})$ tends to suppress this order. The interaction $J(\text{Cu-Co})$ is on the same order as $J(\text{Co-Co})$ at $c \approx 0.51$, increases with increasing concentration and becomes on the same order as $|J(\text{Cu-Cu})|$ at $c \approx 0.83$. We also note that the probability of finding Cu-Co pairs is larger than that of finding Co-Co pairs and Cu-Cu pairs for $0.33 < c < 0.67$. The probability of finding each bond is given by $p(\text{Cu-Cu})=c^2$, $p(\text{Cu-Co})=2c(1-c)$, and $p(\text{Co-Co})=(1-c)^2$. Thus it is concluded that the ferromagnetic long-range order observed for $c > 0.5$ is due mainly to the ferromagnetic interaction $J(\text{Cu-Co})$.

The ac magnetic susceptibility of stage-2 $\text{Cu}_c\text{Co}_{1-c}\text{Cl}_2$ GIC's with $c=0, 0.1, 0.2, 0.4, 0.5, 0.6, 0.7, 0.75, 0.8,$

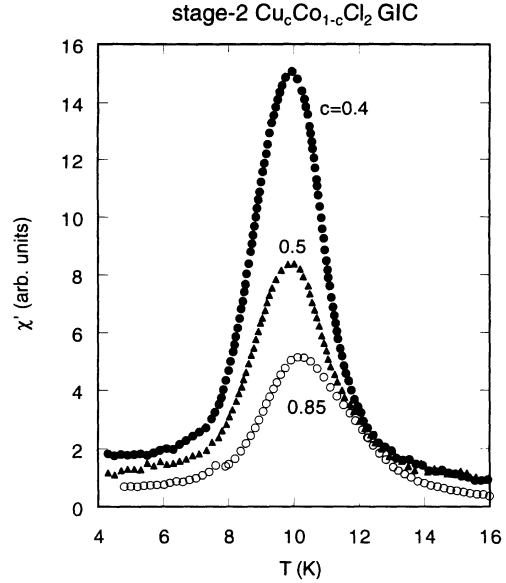


FIG. 5. Temperature dependence of ac magnetic susceptibility for stage-2 $\text{Cu}_c\text{Co}_{1-c}\text{Cl}_2$ GIC's with $c=0.4, 0.5,$ and 0.85 .

$0.85, 0.87, 0.88,$ and 0.9 was measured in the temperature range between 4.2 and 20 K. Figure 5 shows the temperature dependence of ac magnetic susceptibility for stage-2 $\text{Cu}_c\text{Co}_{1-c}\text{Cl}_2$ GIC's with $c=0.4, 0.5,$ and 0.85 . The ac magnetic susceptibility for stage-2 $\text{Cu}_c\text{Co}_{1-c}\text{Cl}_2$ GIC's with $c \leq 0.85$ shows a very sharp peak at the critical temperature T_c below which a ferromagnetic long-range order appears. On the other hand, the ac magnetic susceptibility shows a very broad peak at T_c for $0.87 \leq c \leq 0.90$, and has no peak at any temperature for $c > 0.9$. The

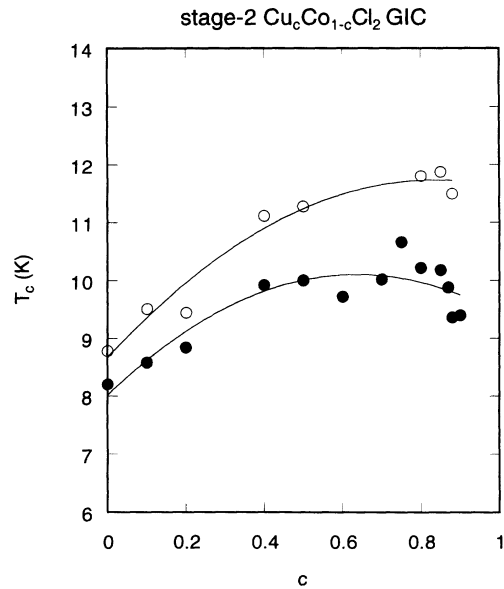


FIG. 6. Critical temperature vs Cu concentration c in stage-2 $\text{Cu}_c\text{Co}_{1-c}\text{Cl}_2$ GIC's determined from ac magnetic susceptibility and dc magnetic susceptibility. The closed circles denote T_c obtained from ac magnetic susceptibility, and the open circles denote $\langle T_c \rangle$ obtained from dc magnetic susceptibility. The solid lines are guide to the eyes.

value of T_c for each concentration is listed in Table II. This disappearance of phase transition in the system with $c > 0.9$ may be ascribed to the spin frustration effects arising from (i) the competition between antiferromagnetic $J(\text{Cu-Cu})$ and ferromagnetic $J(\text{Cu-Co})$, and (ii) the frustrated nature of the 2D antiferromagnet on the isosceles triangular lattice. Figure 6 shows the Cu concentration dependence of T_c denoted by closed circles and $\langle T_c \rangle$ denoted by open circles for stage-2 $\text{Cu}_c\text{Co}_{1-c}\text{Cl}_2$ GIC's, where T_c and $\langle T_c \rangle$ were determined from ac magnetic susceptibility and dc magnetic susceptibility measurements, respectively. The value of T_c is a little lower than that of $\langle T_c \rangle$. We think that T_c corresponds to a real critical temperature. The initial slope defined by $d(\ln T_c)/dc$ at $c=0$ is estimated as 0.46 ± 0.06 . The value of T_c in both the intermediate concentration range

of $0.4 < c \leq 0.8$ is larger than that of T_c in the low concentration range of $0 \leq c \leq 0.2$ and the high concentration range of $0.8 < c \leq 0.9$. As will be discussed in Sec. IV, the enhancement of T_c for intermediate concentration is due to the ferromagnetic interaction $J(\text{Cu-Co})$. The value of $J(\text{Cu-Co})$ is much larger than that of $J(\text{Co-Co})$, which is responsible for the ferromagnetic long-range spin order of the systems with low concentrations.

The temperature dependence of SQUID magnetization M_{ZFC} and M_{FC} for stage-2 $\text{Cu}_c\text{Co}_{1-c}\text{Cl}_2$ GIC's with $c=0, 0.8, 0.87, \text{ and } 0.90$ was measured in the temperature range between 2 and 20 K, where M_{ZFC} and M_{FC} are defined in Sec. II. A magnetic field of 1 Oe was applied along any direction perpendicular to the c axis. Figure 7 shows the temperature dependence of M_{ZFC} , M_{FC} , and the difference $\delta (=M_{\text{FC}} - M_{\text{ZFC}})$ for stage-2 $\text{Cu}_c\text{Co}_{1-c}\text{Cl}_2$

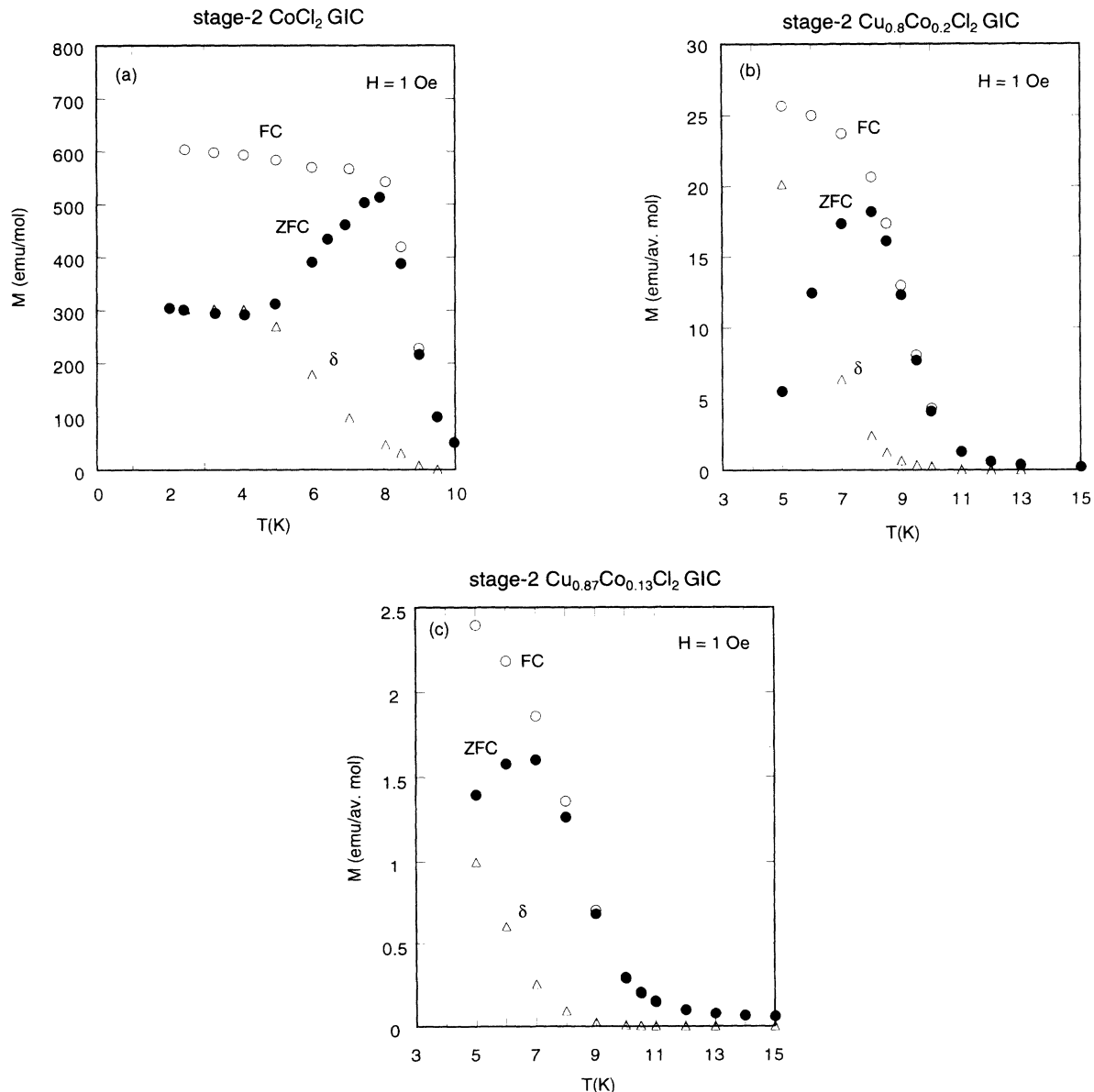


FIG. 7. Temperature dependence of SQUID magnetization in stage-2 $\text{Cu}_c\text{Co}_{1-c}\text{Cl}_2$ GIC's with (a) $c=0$, (b) $c=0.80$, and (c) $c=0.87$. M_{ZFC} and M_{FC} denote the zero-field-cooled, and field-cooled magnetization, respectively: $\delta = M_{\text{FC}} - M_{\text{ZFC}}$.

GIC's with (a) $c=0$, (b) $c=0.8$, and (d) $c=0.87$. For each Cu concentration, M_{ZFC} shows a broad peak at a temperature denoted by T_{max} . As will be discussed later, this peak in M_{ZFC} implies that there exist ferromagnetic clusters in the intercalate layers. The magnetization M_{ZFC} coincides with M_{FC} at sufficiently high temperatures and begins to deviate downward from M_{FC} at a critical temperature T_c below which δ is not equal to zero. The difference δ increases monotonically with decreasing temperature for any Cu concentration, and does not show any anomaly around T_{max} . The difference δ is a measure of spin frustration effect occurring in the system, and is usually observed in spin glasses where the ground state has a multivalley structure with degenerate states. The difference δ implies that spin frustration effects exist in these systems. The magnetization M_{FC} increases rapidly with decreasing temperature below T_c similar to a spontaneous magnetization of the usual ferromagnet. We note that the value of M_{FC} at 5 K decreases drastically from $M_{FC}=600$ (emu/mol) to 2.5 (emu/av mol) as the Cu concentration varies from $c=0$ to 0.87. The values of T_c and T_{max} for each Cu concentration are derived from the temperature variation of δ and M_{ZFC} , respectively: $T_c=9.5$ K and $T_{max}=7.8$ K for $c=0$, $T_c \approx 10$ K and $T_{max}=8.0$ K for $c=0.8$, and $T_c \approx 9$ K and $T_{max}=7.0$ K for $c=0.87$. Note that these values of T_c are not so accurate as those determined from ac magnetic susceptibility measurements due to limited data.

IV. DISCUSSION

In stage-2 $Cu_cCo_{1-c}Cl_2$ GIC's the spin frustration effect is considered to occur as a result of competition between ferromagnetic $J(\text{Co-Co})$ and $J(\text{Cu-Co})$ interactions and antiferromagnetic $J(\text{Cu-Cu})$, and competition between XY symmetry from Co^{2+} spins and Heisenberg symmetry from Cu^{2+} spins. Furthermore, stage-2 $CuCl_2$ GIC has the fully frustrated nature of a 2D antiferromagnet on a triangular lattice. As far as we know, there has been no theory for the concentration dependence of T_c in such a complicated system. Here we discuss the concentration dependence of T_c in stage-2 $Cu_cCo_{1-c}Cl_2$ GIC's in terms of the molecular field approximation. In this approximation, the critical temperature T_c coincides with the Curie-Weiss temperature Θ defined by Eq. (3). Experimentally the value of T_c is much lower than that of Θ , indicating that the molecular field approximation is not a good one for the discussion of T_c because the spin fluctuation effect is not taken into account. In spite of this fact, it is interesting to compare our data of T_c vs c with the curve of Θ vs c calculated by Eq. (3) with $\alpha=0, 1$, and 2. For $\alpha=2$, as shown in Fig. 3(a), the value of Θ increases with increasing concentration from $c=0$ to 0.4, showing a broad peak between $c=0.4$ and 0.5, and then decreasing. Such a temperature dependence is similar to our data of T_c vs c at least for $0 \leq c \leq 0.6$. For $\alpha=0$ and 1, the value of Θ monotonically decreases with increasing concentration. These results suggest that the broad peak of T_c observed for intermediate concentration is due to the ferromagnetic $J(\text{Cu-Co})$ interaction with relatively large α .

Next we discuss the origin of this ferromagnetic $J(\text{Cu-Co})$ interaction. The exchange interaction $J(\text{Cu-Co})$ between Cu^{2+} and Co^{2+} ions is a superexchange interaction through the Cl^- ions.²⁴ This superexchange interaction is considered to depend strongly on the distance between Cu^{2+} and Cl^- , the distance between Co^{2+} and Cl^- , and angle between Cu-Cl and Co-Cl bonds. In stage-2 $Cu_cCo_{1-c}Cl_2$ GIC's the intercalate layer formed of Cu_cCo_{1-c} is sandwiched between upper and lower Cl layers. The separation distance between the Cu_cCo_{1-c} intercalate layer and the Cl layer is given by z_1 . For stage-2 $CuCl_2$ GIC the separation distance z_1 is described in terms of sides a_1 and a_2 as

$$z_1 = \frac{a_1}{\sqrt{2}} \left[\frac{2a_2^2 - a_1^2}{4a_2^2 - a_1^2} \right]^{1/2}, \quad (6)$$

which is equal to 1.43 Å.¹⁸ Each Cu^{2+} ion in stage-2 $CuCl_2$ GIC is located at the center of distorted octahedron consisting of six Cl^- ions. The nearest-neighbor distance between the Cu^{2+} and Cl^- ions in the tetragonal plane calculated as $a_{NN}=a_1/\sqrt{2}$ ($=2.33$ Å) is shorter than the distance between the Cu^{2+} and Cl^- ions along the tetragonal axis calculated as $a_{NNN}=[a_2^2 - (1/2)a_1^2]^{1/2}$ ($=2.90$ Å). The bond between a Cu^{2+} ion and a Cl^- ion separated by a_{NN} is perpendicular to that between the nearest-neighbor Cu^{2+} ion and the same Cl^- ion separated by a_{NN} . Furthermore, the bond between a Cu^{2+} ion and a Cl^- ion separated by a_{NNN} is also perpendicular to that between the next-nearest-neighbor Cu^{2+} ion and the same Cl^- ion separated by a_{NN} . In stage-2 $CoCl_2$ GIC, the Co^{2+} ions form a triangular lattice with side a ($=3.55$ Å). Each Co^{2+} ion of stage-2 $CoCl_2$ GIC is located at the center of an octahedron consisting of six Cl^- ions.⁶ The distance z_1 is related to side a as $z_1=a/\sqrt{6}$ ($=1.45$ Å), and the nearest-neighbor distance between the Co^{2+} ion and the Cl^- ion is given by $a_{NN}=a/\sqrt{2}$ ($=2.51$ Å). The bond between a Co^{2+} ion and a Cl^- ion separated by a_{NN} is perpendicular to that between the nearest-neighbor Co^{2+} and the same Cl^- ion separated by a_{NN} . In the stage-2 $Cu_cCo_{1-c}Cl_2$ GIC's the distance between the Cu^{2+} ion and the Cl^- ion, and the distance between the Co^{2+} ion and the Cl^- ion may change with concentration, but the angle between the Cu-Cl bond and Co-Cl bond is assumed to be independent of concentration and to be equal to $\phi=90^\circ$.

An empirical rule (Goodenough-Kanamori²⁵) is well established for determining the sign of the superexchange interaction from the symmetry relation between the occupied d orbitals ($d\epsilon$ and $d\gamma$) and occupied p orbitals (p_σ and p_π) for bulk transition metal dichlorides. The p_σ orbital is orthogonal to the $d\epsilon$ orbital, indicating that the exchange interaction between $d\epsilon$ and p_σ is ferromagnetic. No charge transfer occurs from the p_σ orbital to the $d\epsilon$ orbital. The p_σ orbital is nonorthogonal to the $d\gamma$ orbital. The p_σ orbital forms a partially covalent bond with the $d\gamma$ orbital. The charge transfer occurs from the p_σ orbital to the $d\gamma$ orbital. The exchange interaction between the p_σ orbital and $d\gamma$ orbital is antiferromagnetic.

Similarly the p_π orbital is orthogonal to the $d\gamma$ orbital. There is no charge transfer between the p_π orbital and the $d\gamma$ orbital. The exchange interaction between the p_π orbital and the $d\gamma$ orbital is ferromagnetic. The p_π orbital is nonorthogonal to the $d\varepsilon$ orbital. There is a charge transfer from the p_π orbital to the $d\varepsilon$ orbital. The exchange interactions between the p_π orbital and the $d\varepsilon$ orbital is antiferromagnetic. The bond between $d\varepsilon$ and p_π should be weaker than that between $d\gamma$ and p_σ due to a smaller overlap of wave functions.

The origin of ferromagnetic $J(\text{Cu-Co})$ may be explained in terms of this Goodenough-Kanamori rule for the $\phi=90^\circ$ case, where the Cu-Cl bond is perpendicular to the Co-Cl bond. The electron configurations of the lowest orbital states of Cu^{2+} and Co^{2+} , which are subject to an octahedral field are given by $(d\varepsilon^6)(d\gamma^2)d\gamma^1$ and $(d\varepsilon^4)d\varepsilon^1d\gamma^2$, respectively, where those in parentheses indicate paired electrons. The Cl^- ion has two electrons with spins up and down. There is some probability that less than one electron is transferred from the p_σ orbital of Cl^- to $d\gamma$ orbital of Cu^{2+} because the p_σ orbital forms a partially covalent bond with the $d\gamma$ orbital. The electron left behind on the Cl^- ion has its spin parallel to the spin of the Cu^{2+} ion. Since the p_σ orbital of the Cl^- ion is orthogonal to the $d\gamma'$ orbital of the Co^{2+} ion, the direct exchange interaction between the remaining unpaired spin on the Cl^- ion and the Co^{2+} spins is ferromagnetic. This implies that the exchange interaction between Cu^{2+} and Co^{2+} spins is ferromagnetic.

Finally we discuss the magnetic phase transition of stage-2 $\text{Cu}_c\text{Co}_{1-c}\text{Cl}_2$ GIC's for $c < 0.87$. The irreversible effect of magnetization observed in stage-2 $\text{Cu}_c\text{Co}_{1-c}\text{Cl}_2$ GIC's with $c < 0.87$ is very similar to that in stage-2 $\text{Co}_c\text{Ni}_{1-c}\text{Cl}_2$ GIC's ($0 \leq c \leq 1$), stage-2 $\text{Co}_c\text{Mn}_{1-c}\text{Cl}_2$ GIC's ($0.9 \leq c \leq 1$), and stage-2 $\text{Co}_c\text{Ni}_{1-c}\text{Cl}_2$ GIC's ($0.8 \leq c \leq 1$),³ where ferromagnetic intraplanar exchange interactions are dominant. We have shown in a previous paper³ that a cluster glass phase below T_c is the cause of the irreversible effect of magnetization in stage-2 $\text{Co}_c\text{Ni}_{1-c}\text{Cl}_2$ GIC's ($0 \leq c \leq 1$), stage-2 $\text{Co}_c\text{Mn}_{1-c}\text{Cl}_2$ GIC's ($0.9 \leq c \leq 1$), and stage-2 $\text{Co}_c\text{Ni}_{1-c}\text{Cl}_2$ GIC's ($0.8 \leq c \leq 1$). These results indicate that a cluster glass phase also occurs below T_c in stage-2 $\text{Cu}_c\text{Co}_{1-c}\text{Cl}_2$ GIC's with $c < 0.87$. The intercalate layers of stage-2 $\text{Cu}_c\text{Co}_{1-c}\text{Cl}_2$ GIC's are considered to be formed of small islands. The periphery of small islands provides acceptor sites for electrons transferred from graphite layers. The diameter of these small islands is on the order of 500 Å for stage-2 CoCl_2 GIC. This cluster glass phase is a type of spin-glass phase where the ground state has a multivalley structure with degenerate states. Below T_c the ferromagnetic spin order is established within each island, forming a ferromagnetic cluster. The spin directions of these ferromagnetic clusters are frozen because of frustrated interisland interactions such as (i) the effective interplanar antiferromagnetic interaction between ferromagnetic clusters of the adjacent intercalate layers and (ii) the dipole-dipole interaction between ferromagnetic clusters in the same intercalate layer. The effective interplanar interaction is dominant to the frustrated interis-

land interaction if the radius of island R is much larger than a characteristic radius R_0 ,³ which depends on the average intraplanar ferromagnetic interaction and the antiferromagnetic interplanar exchange interaction J' . On the other hand, the dipole-dipole interaction is dominant to the frustrated interisland interaction if R is much smaller than R_0 . Since the value of R_0 is estimated to be on the same order as R in stage-2 CoCl_2 GIC's, it may be concluded that both the dipole-dipole interaction and the effective interplanar interaction contribute to the frustrated interisland interaction for stage-2 $\text{Cu}_c\text{Co}_{1-c}\text{Cl}_2$ GIC's. The temperature dependence of ZFC magnetization around T_{max} can be qualitatively explained as follows. The thermal energy, which increases with increasing temperature becomes comparable to the frustrated interisland interaction at T_{max} . Above T_{max} this thermal energy overcomes the frustrated interisland interaction, and the spin direction of ferromagnetic clusters becomes random. Above T_c , the direction of each spin in the ferromagnetic cluster becomes random.

V. CONCLUSION

We have studied the magnetic properties of stage-2 $\text{Cu}_c\text{Co}_{1-c}\text{Cl}_2$ GIC's. This is the first time these GIC's have ever been successfully fabricated and analyzed. These compounds provide a model system for studying the phase transition of spin frustrated systems having a competition between ferromagnetic and antiferromagnetic interactions. Because of the strong ferromagnetic $J(\text{Cu-Co})$ interaction, these systems (when $c < 0.9$) undergo a ferromagnetic phase transition at a critical temperature T_c . The low-temperature phase below T_c is considered to be a cluster glass phase, where the spin direction of ferromagnetic clusters is frozen because of frustrated interisland interaction. In the system with $c \approx 0.9$ one may expect that a competition between ferromagnetic $J(\text{Cu-Co})$ and antiferromagnetic $J(\text{Cu-Cu})$ gives rise to a spin-glass phase, where the direction of each spin is frozen below T_c . In this case the magnetization M_{ZFC} is assumed to show no peak below T_c . Magnetic neutron scattering studies show that stage-2 CuCl_2 GIC does not show any magnetic phase transition down to 0.3 K. This may be partly due to the spin frustration effect arising from the fully frustrated nature of antiferromagnetism on the triangular lattice.

ACKNOWLEDGMENTS

We would like to thank H. Suematsu and Y. Hishiyama for providing us with high-quality single-crystal kish graphite and A. Moore for providing highly oriented pyrolytic graphite. We would like to thank Y. Maruyama for providing us with the opportunity to use the SQUID magnetometer facility at the Institute for Molecular Science, Japan. We are also grateful to E. Piscani, C. Vartuli, J. Fu, F. Khemai, T. Mellin, N. Inadama, J. Wilson, and W. Brinkman for their help with sample preparation, x-ray scattering and dc magnetic susceptibility measurements. This work was supported by NSF Grant No. DMR 9201656.

- ¹M. Yeh, I. S. Suzuki, M. Suzuki, and C. R. Burr, *J. Phys. Condens. Matter* **2**, 9821 (1990).
- ²M. Suzuki, I. S. Suzuki, W. Zhang, and C. R. Burr, *Phys. Rev. B* **46**, 5311 (1992).
- ³I. S. Suzuki, M. Suzuki, and Y. Maruyama, *Phys. Rev. B* **48**, 13 550 (1993).
- ⁴I. S. Suzuki, M. Suzuki, L.F. Tien, and C. R. Burr, *Phys. Rev. B* **43**, 6393 (1991).
- ⁵I. S. Suzuki, F. Khemai, M. Suzuki, and C. R. Burr, *Phys. Rev. B* **45**, 4721 (1992).
- ⁶J. T. Nicholls and G. Dresselhaus, *Phys. Rev. B* **41**, 9744 (1990).
- ⁷I.S. Suzuki, Chi-Jen Hsieh, F. Khemai, C. R. Burr, and M. Suzuki, *Phys. Rev. B* **47**, 845 (1993).
- ⁸M. Suzuki, *Crit. Rev. Solid State Mater. Sci.* **16**, 237 (1990).
- ⁹G. Dresselhaus, J. T. Nicholls, and M. S. Dresselhaus, in *Graphite Intercalation Compounds II*, edited by H. Zabel and S. A. Solin (Springer-Verlag, New York, 1992), p. 247.
- ¹⁰D. G. Wiesler, M. Suzuki, P. C. Chow, and H. Zabel, *Phys. Rev. B* **34**, 7951 (1986).
- ¹¹D. G. Wiesler, M. Suzuki, and H. Zabel, *Phys. Rev. B* **36**, 7051 (1987).
- ¹²D. G. Wiesler, H. Zabel, and S. M. Shapiro, *Z. Phys. B* **93**, 277 (1994).
- ¹³C. Hauw, J. Gaultier, S. Flandrois, O. Gonzalez, O. Dorignac, and R. Jagut, *Synth. Met.* **7**, 313 (1983).
- ¹⁴H. Nishihara, I. Oguro, M. Suzuki, K. Koga, and H. Yasuoka, *Synth. Met.* **12**, 473 (1985).
- ¹⁵K. Koga, M. Suzuki, and H. Yasuoka, *Synth. Met.* **12**, 467 (1985).
- ¹⁶D. G. Rancourt, C. Meschi, and S. Flandrois, *Phys. Rev. B* **33**, 347 (1986).
- ¹⁷J. S. Speck, J. T. Nicholls, B. J. Wuensch, J. M. Delgado, and M. S. Dresselhaus, *Philos. Mag. B* **64**, 181 (1991).
- ¹⁸M. Suzuki, I. S. Suzuki, C. R. Burr, D. G. Wiesler, N. Rosov, and K. Koga (unpublished).
- ¹⁹S. Hendricks and E. Teller, *J. Chem. Phys.* **10**, 147 (1942).
- ²⁰I. S. Suzuki and M. Suzuki, *J. Phys. Condens. Matter* **3**, 8825 (1991).
- ²¹F. Horzberg, T. R. McGuire, S. Methfessel, and J. C. Suits, *Phys. Rev. Lett.* **13**, 18 (1964).
- ²²M. F. Collins, *Magnetic Critical Scattering* (Oxford University Press, Oxford, England, 1989).
- ²³R. B. Stinchcombe, in *Phase Transitions and Critical Phenomena*, edited by C. Domb and J. L. Lebowitz (Academic, New York, 1983), Vol. 7, p. 152.
- ²⁴P. W. Anderson, in *Solid State Physics*, edited by F. Seitz and D. Turnbull (Academic, New York, 1963), Vol. 14, p. 99.
- ²⁵J. Kanamori, *J. Phys. Chem. Solid* **10**, 87 (1959).